

Multi-Level Attention Pooling for Graph Neural Networks: Unifying Graph Representations with Multiple Localities

Takeshi D. Itoh, Takatomi Kubo*, Kazushi Ikeda

Division of Information Science, Graduate School of Science and Technology, Nara Institute of Science and Technology, 8916-5 Takayama-Cho, Ikoma, Nara 630-0192, Japan

Abstract

Graph neural networks (GNNs) have been widely used to learn vector representation of graph-structured data and achieved better task performance than conventional methods. The foundation of GNNs is the message passing procedure, which propagates the information in a node to its neighbors. Since this procedure proceeds one step per layer, the range of the information propagation among nodes is small in the lower layers, and it expands toward the higher layers. Therefore, a GNN model has to be deep enough to capture global structural information in a graph. On the other hand, it is known that deep GNN models suffer from performance degradation because they lose nodes' local information, which would be essential for good model performance, through many message passing steps. In this study, we propose a multi-level attention pooling (MLAP) for graph-level classification tasks, which can adapt to both local and global structural information in a graph. It has an attention pooling layer for each message passing step and computes the final graph representation by unifying the layer-wise graph representations. The MLAP architecture allows models to utilize the structural information of graphs with multiple levels of localities because it preserves layer-wise information before losing them due to oversmoothing. Results of our experiments show that the MLAP architecture improves deeper models' performance in graph classification tasks compared to the baseline architectures. In addition, analyses on the layer-wise graph representations suggest that aggregating information from multiple levels of localities indeed has the potential to improve the discriminability of learned graph representations.

Keywords: Graph representation learning (GRL), Graph neural network (GNN), Multi-level attention pooling (MLAP), Multi-level locality

1. Introduction

Graph-structured data are found in many fields. A wide variety of natural and artificial objects can be expressed with graphs, such as molecular structural formula, biochemical reaction pathways, brain connection networks, social networks, and abstract syntax trees of computer programs. Because of this ubiquity, machine learning methods on graphs have been actively studied. Thanks to rich information underlying the structure, graph machine learning techniques have shown remarkable performances in various tasks. For example, the PageRank algorithm (Page et al., 1999) computes the importance of each node in a directed graph based on the number of inbound edges to the node. Shervashidze et al. (2011) used a graph kernel method (Kondor & Lafferty, 2002) to predict chemical molecules' toxicity as a graph classification task. Despite these promising applications, classical machine learning

techniques on graphs require difficult and costly processes for manually designing features or kernel functions.

In contrast to those classical graph machine learning methods using hand-crafted features, recent years have witnessed a surge in graph representation learning (GRL; Hamilton et al., 2017a). A GRL model learns a mapping from a node or a graph to a vector representation. The mapping is trained so that the geometric relationships among embedded representations reflect the similarity of structural information in graphs, *i.e.*, nodes with similar local structures have similar representations (Belkin & Niyogi, 2001; Ahmed et al., 2013). The representation provided by the mapping can then be used as an input feature for task-specific models, such as classifiers or regressors. Graph features *learned* by GRL are more flexible than the *hand-crafted* features used in classical graph machine learning methods. However, the early GRL techniques learned a unique vector for each node without sharing parameters among nodes, leading to high computational costs and the risk of overfitting. Furthermore, since these techniques learn a specific representation for each node, learned models cannot be applied for prediction on novel graphs or nodes that do not appear in the training

*Corresponding author.

Email addresses: itoh.takeshi.ik4@is.naist.jp (Takeshi D. Itoh), takatomi-k@is.naist.jp (Takatomi Kubo), kazushi@is.naist.jp (Kazushi Ikeda)

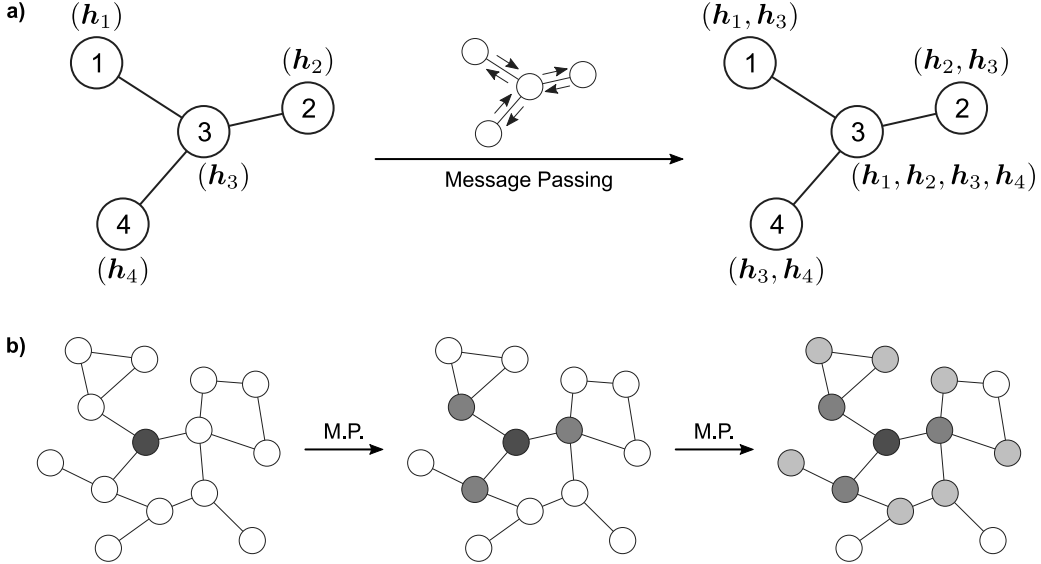


Figure 1: **a)** A schematic illustration of the message passing procedure. i -th node has its original node information, \mathbf{h}_i ($i = 1, \dots, 4$), at the beginning (left). The message passing procedure propagates node information between each pair of connected nodes (center). As a result, each node has its own information and neighbor information after the message passing (right). **b)** The scope of the information propagation expands along the message passing process. The black node in the middle of a graph has only its original node information at the beginning (left). This node obtains information in broader subgraphs through message passing, *i.e.*, dark gray nodes after one message passing step (center) and light gray nodes after two message passing steps (right). *M.P.*: message passing.

phase (Hamilton, 2020, Section 3.4).

More recently, graph neural networks (GNNs) has rapidly emerged as a new framework for GRL (we refer readers to Zhang et al. 2018b and Wu et al. 2021 for review papers; see Section 2 for related works). Unlike (non-GNN) GRL techniques which learn node-specific representations, GNNs learn how to compute the node representation from the structural information around a node. Hence, GNNs do not suffer from the problem that the computation cost increases linearly to the number of nodes. Furthermore, the learned models generalize to the graphs or nodes which are unknown while training. The foundation of GNNs is the message passing procedure that propagates the information in a node to its neighbor nodes, each of which is directly connected to the source node by an edge (Fig. 1a; see Section 3.1 for detail). Since this procedure proceeds one step per layer, the range of the information propagation among nodes is small in the lower layers, and it expands toward the higher layers—*i.e.*, the node representations in the higher layers collect information from broader subgraphs (Fig. 1b).

However, there is a problem in GNNs that the model performance degrades as the number of layers increases. This is because deep GNN models lose the nodes’ local information, which would be essential for good model performances, through many message passing steps. This phenomenon is known as *oversmoothing* (Li et al., 2018). Many real-world graphs have fractal characteristics (Kim et al., 2007). Therefore, a GRL model needs to be capable of capturing both local structural information and global structural information. Capturing global structural

information requires a GNN model to be deep (*i.e.*, having many message passing steps), but the oversmoothing problem prevents GNN models from getting deep.

In this study, we focus on improving learned graph representations for graph-level prediction tasks, such as molecular property classification. Specifically, we seek a technique to learn more discriminative graph representation by using multiple representations in different localities. Previous studies typically computed the graph representation by a graph pooling layer that collects node representations after the last message passing layer. Therefore, deeper models cannot utilize nodes’ local information in computing the graph representation because local information is lost through many message passing steps due to oversmoothing. There are many prior works tackling the oversmoothing problem (see Section 2.2). On the other hand, our approach—using information with multiple levels of localities to compute graph representations—does not aim to directly solve the oversmoothing problem itself, but we focus on improving the discriminability of learned representations. To this end, we propose a multi-level attention pooling (MLAP) architecture. In short, the MLAP architecture introduces an attention pooling layer (Li et al., 2016) for each message passing step to compute layer-wise graph representations. Then, it aggregates them to compute the final graph representation, inspired by the jumping knowledge network (Xu et al., 2018). Doing so, the MLAP architecture can focus on different nodes (or different subgraphs) in each layer with a different levels of information localities, which leads to better modeling of both local structural information and

global structural information. In other words, introducing layer-wise attention pooling *prior to* aggregating layer-wise representation would improve the graph-level classification performance. Our experiments showed performance improvements in deeper GNN models with the MLAP architecture. In addition, analyses on the layer-wise graph representations suggest that MLAP has the potential to learn graph representations with improved class discriminability by aggregating information with multiple levels of localities.

Our contributions in this works are following.

- We propose the MLAP architecture for GNNs, which uses an attention-based global graph pooling (Li et al., 2016) for each message passing layer and the aggregation mechanism of layer-wise representations (Xu et al., 2018) in combination.
- Our experiments show that GNN models with MLAP architecture demonstrate better graph classification performance in multiple datasets.
- We also empirically show that aggregating information in different levels of localities has the potential to improve the discriminability of the learned graph representation.

The rest of this paper is organized as follows: Section 2 summarizes related works, Section 3 introduces the proposed MLAP framework, Section 4 describes the experimental setups, Section 5 demonstrates the results, Section 6 discusses the results, and Section 7 concludes the present study.

2. Related Works

Gori et al. (2005) and Scarselli et al. (2009) first introduced the idea of GNNs, and Bruna et al. (2014) and Defferrard et al. (2016) elaborated the formulation in the graph Fourier domain using spectral filtering. Based on these earlier works, Kipf & Welling (2017) proposed the graph convolution network (GCN), which made a foundation of today’s various GNN models (Duvenaud et al., 2015; Hamilton et al., 2017b; Niepert et al., 2016; Veličković et al., 2018; Xu et al., 2019). Gilmer et al. (2017) summarized these methods as a framework named neural message passing, which computes node representations iteratively by collecting neighbor nodes’ representation using differentiable functions.

In this study, we focus on methods to compute the graph representation from node-wise representations in GNN models. We first summarize the studies on graph pooling methods and then review the recent trends in *deep* GNN studies. Finally, we summarize prior works that aggregate layer-wise representation to compute the final node/graph representation and elaborate the idea behind our proposed method.

2.1. Graph Pooling Methods

Techniques to learn *graph* representations are usually built upon those to learn *node* representations. A graph-level model first computes the representation for each node in a graph and then collects the node-wise representations into a single graph representation vector. This collection procedure is called a pooling operation. Although there are various pooling methods, they fall into two categories: the *global* pooling approach and the *hierarchical* pooling approach.

The *global* pooling approach collects all of the node representations in a single computation. The simplest example of the global pooling method is sum pooling, which merely computes the sum of all node representations. Duvenaud et al. (2015) introduced sum pooling to learn embedded representations of molecules from a graph where each node represents an atom. Likewise, one can compute an average or take the maximum elements as a pooling method. Li et al. (2016) introduced attention pooling, which computes a weighted sum of node representations based on a softmax attention mechanism (Bahdanau et al., 2015). Vinyals et al. (2016) proposed set2set by extending the sequence to sequence (seq2seq) approach for a set without ordering. Zhang et al. (2018a) introduced the SortPooling, which sorts the node representations regarding their topological features and applies one-dimensional convolution. These global pooling methods are simple and computationally lightweight, but they cannot use the structural information of graphs in the pooling operation.

In contrast, *hierarchical* pooling methods segment the entire graph into a set of subgraphs hierarchically and compute the representations of subgraphs iteratively. Bruna et al. (2014) introduced the idea of hierarchical pooling, or graph coarsening, based on hierarchical agglomerative clustering. Although some early works like Defferrard et al. (2016) also applied similar approaches, such clustering-based hierarchical pooling requires the clustering algorithm to be deterministic—that is, the hierarchy of subgraphs is fixed throughout the training. To overcome this limitation, Ying et al. (2018) proposed DiffPool, which learns the subgraph hierarchy itself along with the message passing functions. They proposed to use a neural network to estimate which subgraph a node should belong to in the next layer. Gao & Ji (2019) extended U-Net (Ronneberger et al., 2015) for graph structure to propose graph U-Nets. Original U-Net introduced down-sampling and up-sampling procedures for semantic image segmentation tasks. Based on the U-Net, graph U-Nets is composed of a gPool network to shrink the graph size hierarchically and a gUnpool network to restore the original graph structure. Also, Lee et al. (2019) employed a self-attention mechanism to define a hierarchy of subgraph structures. Hierarchical pooling can adapt to multiple localities of graph substructures during step-wise shrinkage of graphs. However, they are often computationally heavy because, as discussed in Cangea et al. (2018), they have to learn the dense “assignment matrix” for each layer, relating a node

in a layer to a node in the shrunk graph in the next layer. Thus, they require longer computational time and consume larger memory.

2.2. Oversmoothing in Deep Graph Neural Networks

Kipf & Welling (2017) first reported that deep GNN models with many message passing layers performed worse than shallower models. Li et al. (2018) investigated this phenomenon and found that deep GNN models converged to an equilibrium point wherein connected nodes have similar representations. Since the nodes with similar representations are indistinguishable from each other, such convergence degrades the performance in node-level prediction tasks. This problem is called *oversmoothing*. In graph-level prediction tasks, oversmoothing occurs independently for each graph. Oversmoothing per graph damages GNN models’ expressivity and results in performance degradation (Oono & Suzuki, 2020).

Studies tackling the oversmoothing problem mainly fall into three categories: modifying the message passing formulation, adding residual connections, or normalization. Anyhow, the objective of those studies is to retain discriminative representations even after many steps of message passing.

Studies modifying the message passing formulation aim to propose techniques to retain high-frequency components in graph signals during message passing steps, whereas message passing among nodes generally acts as a low-pass filter for the signals. Min et al. (2020) proposed scattering GCN, which adds a circuit for band-pass filtering of node representations. DropEdge (Rong et al., 2020) randomly removes some edges from the input graph, alleviating the low-pass filtering effect of the graph convolution. Also, although not explicitly stated, the graph attention network (GAT; Veličković et al., 2018) is known to mitigate the oversmoothing problem because it can focus on specific nodes during message passing.

Adding residual connections is a more straightforward way to retain node-local representation up to deeper layers. Residual connections, or ResNet architecture, were first introduced to convolutional neural networks for computer vision tasks, achieving a state-of-the-art performance (He et al., 2016). Kipf & Welling (2017) applied the residual connections in the graph convolutional network and reported that residual connections mitigated the performance degradation in deeper models. Later, Li et al. (2019), Zhang & Meng (2019), and Chen et al. (2020) applied similar residual architectures on GNNs and showed performance improvement.

Normalization in deep learning gained attention by the success of early works such as BatchNorm (Ioffe & Szegedy, 2015) and LayerNorm (Ba et al., 2016). Although these general normalization techniques are also applicable and effective in GNNs, there are graph-specific normalization methods recently proposed. PairNorm (Zhao & Akoglu, 2020), NodeNorm (Zhou et al., 2020a), GraphNorm (Cai et al., 2020), and differentiable group normalization (DGN;

Zhou et al., 2020b) are representative examples of graph-specific normalization methods.

These studies succeeded in overcoming the oversmoothing problem and make deep GNN models retain discriminative representations. On the other hand, directly using local representations in computing the final graph representation would lead to more performance improvement.

2.3. Aggregating Layer-Wise Representations in GNN

The studies summarized in the previous subsection directly tackle the oversmoothing problem. That is, they sought techniques to retain discriminative representations even after multiple steps of message passing. Instead, we search for a technique to learn more discriminative representation by aggregating multiple representations in different localities.

Jumping knowledge (JK) network (Xu et al., 2018) proposed to compute the final node representation by aggregating intermediate layer-wise node representations. Doing so, JK can adapt the locality of the subgraph from which a node gathers information. After JK was proposed, many studies adopted JK-like aggregation of layer-wise representation to improve the learned representation. Wang et al. (2019) adopted JK in recommendation tasks on knowledge graphs. Cangea et al. (2018) adopted a JK-like aggregation of layer-wise pooled representation upon gPool (Gao & Ji, 2019) network to learn graph-level tasks. A similar combination of hierarchical graph pooling and JK-like aggregation was also proposed by Ranjan et al. (2020). Dehmamy et al. (2019) proposed aggregating layer-wise representation from a modified GCN architecture and showed performance improvement.

Our proposed MLAP technique is motivated by the same idea of these studies that GNNs should be capable of aggregating information in multiple levels of localities. Here, we utilize an intuition on graph-level prediction tasks: a model should focus on different nodes as the message passing proceeds through layers and the locality of information extends. That is, the importance of a node in global graph pooling would differ depending on the locality of the information. Therefore, in this study, we propose a method that uses an attention-based global pooling in each layer and aggregates those layer-wise graph representations to compute the final graph representation.

3. Methods

We propose the MLAP architecture, which aggregates graph representation in multiple levels of localities. In this section, we first summarize the fundamentals of GNNs, particularly the message passing procedure, and then introduce the MLAP architecture.

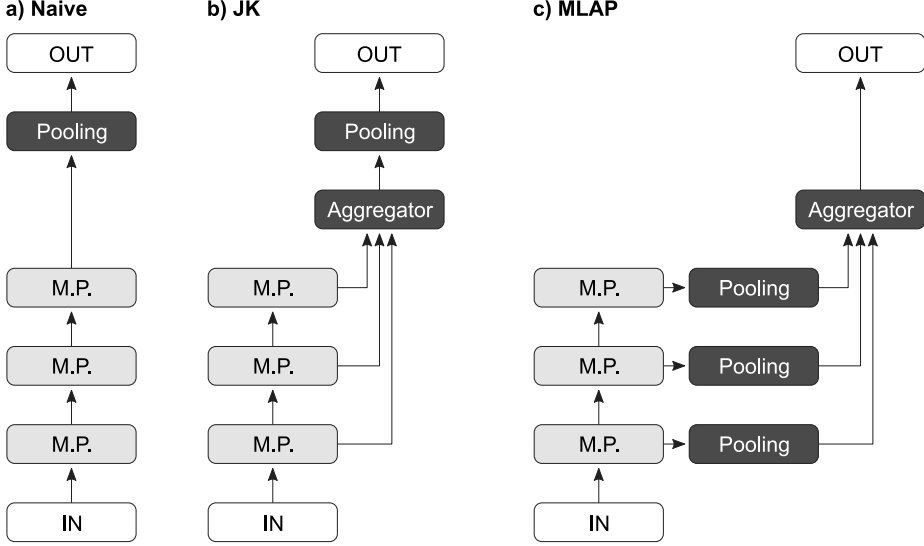


Figure 2: **a)** A naive GNN architecture. A pooling layer computes the graph representation from the node representations after the last message passing. **b)** The jumping knowledge (JK) network architecture. The aggregator collects the layer-wise *node* representation, and then a pooling layer computes the graph representation from the aggregated node representation. **c)** Proposed multi-level attentional pooling (MLAP) architecture. There is a dedicated pooling layer for each message passing layer to compute layer-wise *graph* representation. The aggregator computes the final graph representation. *M.P.*: message passing.

3.1. Preliminaries: Graph Neural Networks

Let $G = (\mathcal{N}, \mathcal{E})$ be a graph, where \mathcal{N} is a set of nodes and \mathcal{E} is a set of edges. $n \in \mathcal{N}$ denotes a node and $e_{n_{\text{src}}, n_{\text{dst}}} \in \mathcal{E}$ denotes a directed edge from a source node n_{src} to a destination node n_{dst} . A graph may have node features or edge features, or both of them. If a graph has node features, each node n has a node feature vector \mathbf{p}_n . Similarly, if a graph has edge features, each edge $e_{n_{\text{src}}, n_{\text{dst}}}$ has an edge feature vector $\mathbf{q}_{n_{\text{src}}, n_{\text{dst}}}$.

There are three types of tasks commonly studied for GNNs: graph-level prediction, node-level prediction, and edge-level prediction. In this study, we focus on the graph-level prediction tasks, that is, given a set of graph $\mathcal{G} = \{G_1, \dots, G_{|\mathcal{G}|}\}$ and their labels $\mathcal{Y} = \{y_1, \dots, y_{|\mathcal{G}|}\}$, we want to learn a graph representation vector \mathbf{h}_G used for predicting the graph label $\hat{y}_G = g(\mathbf{h}_G)$, where g is a predictor function.

Suppose we have a GNN with L layers. Each layer in a GNN propagates the node representation \mathbf{h}_n along the edges (*message passing*). Let $\mathbf{h}_n^{(l)} \in \mathbb{R}^d$ be the representation of n after the message passing by the l -th layer, where d is the dimension of the vector representations. In general, the propagation by the l -th layer first computes the *message* $\mathbf{m}_n^{(l)}$ for each node n from its neighbor nodes $\text{NBR}(n)$, as in

$$\mathbf{m}_n^{(l)} = f_{\text{col}}^{(l)} \left(\left\{ f_{\text{msg}}^{(l)} \left(\mathbf{h}_{n'}^{(l-1)}, \mathbf{q}_{n', n} \right) \mid n' \in \text{NBR}(n) \right\} \right), \quad (1)$$

where $f_{\text{msg}}^{(l)}$ is a message function to compute the message for each neighbor node from the neighbor representation and the feature of the connecting edge, and $f_{\text{col}}^{(l)}$ is a function to collect the neighbor node-wise messages. Then, the

layer *updates* the node representation $\mathbf{h}_n^{(l)}$ as

$$\mathbf{h}_n^{(l)} = f_{\text{upd}}^{(l)} \left(\mathbf{m}_n^{(l)}, \mathbf{h}_n^{(l-1)} \right), \quad (2)$$

where $f_{\text{upd}}^{(l)}$ is an update function.

After L steps of message passing, a graph pooling layer computes a graph representation vector \mathbf{h}_G from the final node representations $\mathbf{h}_n^{(L)}$ for each $n \in \mathcal{N}$, as in

$$\mathbf{h}_G = \text{Pool} \left(\left\{ \mathbf{h}_n^{(L)} \mid n \in \mathcal{N} \right\} \right). \quad (3)$$

3.2. Multi-Level Attentional Pooling

Graph-level prediction tasks require the models to utilize both local information in nodes and global information as the entire graphs for good performances. However, typical GNN implementations first execute the message passing among nodes for a certain number of steps L and then pool the node representations into a graph representation, as shown in Eq. (3) (Fig. 2a). This formulation damages GNN models' expressivity because it can only use the information in a fixed locality to compute the graph representation.

To fix this problem, we introduce a novel GNN architecture named multi-level attentional pooling (MLAP; Fig. 2c). In the MLAP architecture, each message passing layer has a dedicated pooling layer to compute layer-wise graph representations, as in

$$\mathbf{h}_G^{(l)} = \text{Pool}^{(l)} \left(\left\{ \mathbf{h}_n^{(l)} \mid n \in \mathcal{N} \right\} \right) \quad \forall l \in \{1, \dots, L\}. \quad (4)$$

Here, we used the attention pooling (Li et al., 2016) as the

pooling layer. Thus,

$$\mathbf{h}_G^{(l)} = \sum_{n \in \mathcal{N}} \text{softmax} \left(f_{\text{gate}}(\mathbf{h}_n^{(l)}) \right) \mathbf{h}_n^{(l)} \quad (5)$$

$$= \sum_{n \in \mathcal{N}} \frac{\exp \left(f_{\text{gate}}(\mathbf{h}_n^{(l)}) \right)}{\sum_{n' \in \mathcal{N}} \exp \left(f_{\text{gate}}(\mathbf{h}_{n'}^{(l)}) \right)} \mathbf{h}_n^{(l)}, \quad (6)$$

where f_{gate} is a function used for computing the attention score. We used a two-layer neural network.

Then, an aggregation function computes the final graph representation by unifying the layer-wise representations as following:

$$\mathbf{h}_G = f_{\text{agg}} \left(\left\{ \mathbf{h}_G^{(l)} \mid l \in \{1, \dots, L\} \right\} \right), \quad (7)$$

where f_{agg} is an aggregation function. One can use an arbitrary function for f_{agg} . In the present study, we tested two types of the aggregation function: *sum* and *weighted*.

3.2.1. sum

One of the simplest ways to aggregate the layer-wise graph representations is to take the sum of them, as in

$$\mathbf{h}_G = \sum_{l=1}^L \mathbf{h}_G^{(l)}. \quad (8)$$

This formulation expresses an assumption that the representation in each layer is equally important in computing the final graph representation.

3.2.2. Weighted

Each layer-wise representation might have different importance depending on the layer index. If this is the case, taking a weighted sum would be adequate to learn such importance of layers, as in

$$\mathbf{h}_G = \sum_{l=1}^L w^{(l)} \mathbf{h}_G^{(l)}, \quad (9)$$

where $\{w^{(l)} \mid l \in \{1, \dots, L\}\}$ is a trainable weight vector.

4. Experiments

Our experimental evaluation aims to answer these research questions:

- RQ1 Does the MLAP architecture improve the GNN performances in graph classification tasks?
- RQ2 Does aggregating multiple layer-wise representations really improve the discriminability of the final graph representation?

To this end, we conducted experiments using three graph classification datasets: a synthetic dataset and two real-world datasets from the graph property prediction collection in the open graph benchmark (OGB; Hu et al., 2020).

4.1. Synthetic Dataset

We created a synthetic dataset to show the effectiveness of MLAP using multi-level representation in a graph-level classification task. We designed the dataset so that its graph features are represented in both local and global graph structures.

A graph in the dataset consists of six 5-node components: one *center* component surrounded by five *peripheral* components, each of which shares a node with the center component (Fig. 3a). The basic structure of a component is five sequentially connected nodes (Fig. 3b) and has an extra edge. Depending on how the extra edge is appended, there are three types of components (Fig. 3c–e). The class of a graph is determined by the combination of the type of the center component and the type of the peripheral components. Note that the five peripheral components share the same type. Therefore, there are $3 \times 3 = 9$ classes. By this design, accurately classifying the graphs in this dataset requires a model to learn both the local substructures in a graph and the global structure as an entire graph (i.e., the combination of the types of local substructures).

We generated 1,000 unique graphs for each class by randomly appending five edges between arbitrarily selected pairs of nodes. Hence, there are 9,000 instances in the dataset in total, and we applied an 8:1:1 split to provide training, validation, and test sets. Model performance is evaluated by the error rate (1 – Accuracy).

4.2. Real-World Benchmark Datasets

We used the following two datasets from OGB (Hu et al., 2020). For both datasets, we followed the standard dataset splitting procedure provided by the OGB.

4.2.1. ogbg-molhiv

ogbg-molhiv is a dataset for a molecular property prediction task, originally introduced in Wu et al. (2018). Each graph in this dataset represents a molecule. Each node in a graph represents an atom and has a 9-dimensional discrete-valued feature containing the atomic number and other atomic properties. Each edge represents a chemical bond between two atoms and has a 3-dimensional discrete-valued feature containing the bond type and other properties. This dataset has a relatively small sample size (41,127 graphs in total), with 25.5 nodes and 27.5 edges per graph on average. The task is a binary classification to identify whether a molecule inhibits the human immunodeficiency virus (HIV) from replication. Model performance is evaluated by the area under the curve value of the radar operator characteristics curve (ROC-AUC).

4.2.2. ogbg-ppa

The ogbg-ppa dataset contains a set of subgraphs extracted from the protein-protein association network of species in 37 taxonomic groups, originally introduced in Szklarczyk et al. (2018). Each node in a graph represents a protein without node features. Each edge represents an

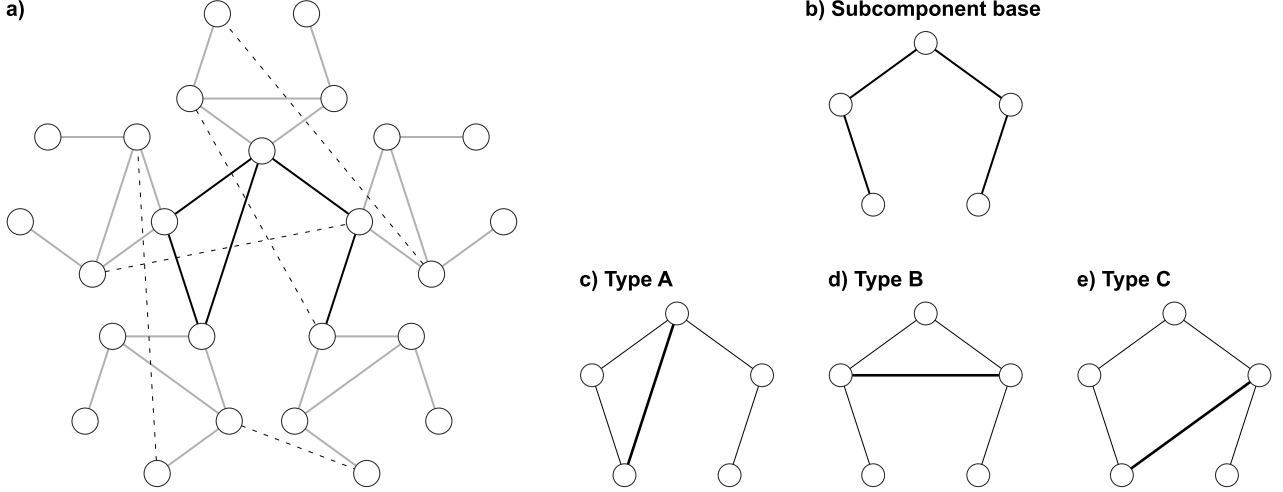


Figure 3: **a)** A graph in the synthetic dataset. It consists of the *center* subcomponent (black edges), five *peripheral* subcomponents (gray edges), and five additional random edges (dotted edges). The class of this graph is determined by the combination of the types of the center component (type A) and the peripheral components (type B). **b)** The basic structure of a subcomponent. **c–e)** Three types of subcomponents.

association between two proteins and has a 7-dimensional real-valued feature describing the biological meanings of the association. This dataset has a medium sample size (158,100 graphs in total), with 243.4 nodes and 2266.1 edges per graph on average. The task is a classification to identify from which taxonomic group among 37 classes an association graph comes. The performance of a model is evaluated by the overall classification accuracy.

4.3. Model Configurations

We used the graph isomorphism network (GIN; Xu et al., 2019) as the message passing layer¹ following the OGB’s reference implementation shown in Hu et al. (2020), *i.e.*, in Eqs. (1) and (2),

$$\mathbf{m}_n^{(l)} = \sum_{n' \in \text{NBR}(n)} \text{ReLU} \left(\mathbf{h}_{n'}^{(l-1)} + f_{\text{edge}}^{(l)}(\mathbf{q}_{n',n}) \right), \quad (10)$$

$$\mathbf{h}_n^{(l)} = f_{\text{NN}}^{(l)} \left((1 + \epsilon^{(l)}) \cdot \mathbf{h}_n^{(l-1)} + \mathbf{m}_n^{(l)} \right), \quad (11)$$

where $f_{\text{edge}}^{(l)}$ is a trainable function to encode edge features into a vector, $f_{\text{NN}}^{(l)}$ is a two-layer neural network for transforming node representations, and $\epsilon^{(l)}$ is a trainable scalar weight modifier.

We varied the number of GIN layers L from 1 to 10 to investigate the effect of depth in model performance. We fixed the node representation dimension d to 200 and added a dropout layer for each GIN layer with a dropout ratio of 0.5. We optimized the model using the Adam optimizer (Kingma & Ba, 2015).

In addition to the bare GIN configuration, we tested the architectures using the GIN + GraphNorm configuration as well, where each GIN layer is followed by GraphNorm (Cai et al., 2020) before dropout.

¹Note that the MLAP architecture is applicable to any GNN models independent of the type of message passing layers.

There are dataset-specific settings detailed below.

4.3.1. Synthetic Dataset

Since the graphs in the synthetic dataset do not have the node features nor edge features, we set $\mathbf{p}_n = 0$ and $\mathbf{q}_{n_{\text{src}}, n_{\text{dst}}} = 0$. Each GIN layer has an edge feature encoder that returns a constant d -dimensional vector.

Besides GNN, each model learned an embedded class representation matrix $\mathbf{E} \in \mathbb{R}^{9 \times d}$. The probability with which a graph belongs to the class c is computed by a softmax function:

$$P(c|G) = \text{softmax}(\mathbf{E}_c \cdot \mathbf{h}_G) = \frac{\exp(\mathbf{E}_c \cdot \mathbf{h}_G + b_c)}{\sum_{c'=1}^9 \exp(\mathbf{E}_{c'} \cdot \mathbf{h}_G + b_{c'})}, \quad (12)$$

where \mathbf{E}_c is the c -th row vector of \mathbf{E} , and b_c is the bias term for the class c .

The models were trained against a cross-entropy loss function for 65 epochs. The initial learning rate was set to 10^{-3} and decayed by $\times 0.2$ for every 15 epochs. The batch size was 50.

4.3.2. ogbg-molhiv

We used the OGB’s atom encoder for computing the initial node representation $\mathbf{h}_n^{(0)}$ from the 9-dimensional node feature. We also used the OGB’s bond encoder as $f_{\text{edge}}^{(l)}$ in Eq. (10), which takes the 3-dimensional edge feature as its input.

After computing the graph representation \mathbf{h}_G by Eq. (8) or Eq. (9), a linear transformation layer followed by a sigmoid function computes the probability with which each graph belongs to the *positive* class, as in

$$P(\text{positive}|G) = \sigma(\mathbf{w}_{\text{prob}} \cdot \mathbf{h}_G + b), \quad (13)$$

where σ is a sigmoid function and \mathbf{w}_{prob} is a trainable row vector with the same dimension d as the graph representation vectors. b is the bias term.

The models were trained against a binary cross-entropy loss function for 50 epochs. The initial learning rate was set to 10^{-4} and decayed by $\times 0.5$ for every 15 epochs. The batch size was set to 20 to avoid overfitting.

4.3.3. ogbg-ppa

We set $\mathbf{p}_n = 0$ because this dataset does not have node features. We used a two-layer neural network as $f_{\text{edge}}^{(l)}$ to embed the edge feature.

The multi-class classification procedure is identical to that used for the synthetic dataset, except that the number of classes is 37. The models were trained against a cross-entropy loss function for 50 epochs. The initial learning rate was set to 10^{-3} and decayed by $\times 0.2$ for every 15 epochs. The batch size was 50.

4.4. Performance Evaluation (RQ1)

4.4.1. Baseline Models

We compared the performance of GNN models with our MLAP framework (Fig. 2c) to two baseline models. One is a naive GNN model that simply stacks GIN layers, wherein the representation of a graph is computed by pooling the node representations after the last message passing (Fig. 2a), as in

$$\mathbf{h}_G = \text{Pool} \left(\left\{ \mathbf{h}_n^{(L)} \mid n \in \mathcal{N} \right\} \right). \quad (14)$$

The other is the JK architecture (Xu et al., 2018), which first computes the final node representations by aggregating layer-wise node representations, and the graph representation is computed by pooling the aggregated node representations (Fig. 2b; Xu et al., 2019), as in

$$\mathbf{h}_G = \text{Pool} \left(\left\{ f_{\text{JK}} \left(\left\{ \mathbf{h}_n^{(l)} \mid l \in \{1, \dots, L\} \right\} \right) \mid n \in \mathcal{N} \right\} \right). \quad (15)$$

Here, f_{JK} is the JK’s aggregation function. We tested all three variants proposed in Xu et al. (2018)—Concatenation, MaxPool, and LSTM-Attention—and *sum* defined as

$$f_{\text{JK}} \left(\left\{ \mathbf{h}_n^{(l)} \mid l \in \{1, \dots, L\} \right\} \right) = \sum_{l=1}^L \mathbf{h}_n^{(l)}, \quad (16)$$

which is used in the OGB’s reference implementation. Those baseline models compute the graph representation using the same pooling function used in MLAP, that is,

$$\mathbf{h}_G = \sum_{n \in \mathcal{N}} \text{softmax} \left(f_{\text{gate}} \left(\mathbf{h}_n^{(L)} \right) \right) \mathbf{h}_n^{(L)}. \quad (17)$$

For each architecture, we trained models with varying depth (1–10). We trained models using 30 different random seeds for the synthetic dataset and 10 seeds for each of the OGB datasets. The performance of an architecture with a certain depth is evaluated by the mean and the standard error.

4.4.2. Statistical Analyses

For each of three datasets and model configuration (*i.e.*, GIN or GIN + GraphNorm), we compared the best performance among MLAP models to naive models and the best JK models using Mann-Whitney U -test. Also, we computed the effect size. Given the test statistic z from the U -test, the effect size r is computed as $r = z/\sqrt{N}$, where N is the total number of samples (*i.e.*, $30 \times 2 = 60$ for the synthetic dataset, or $10 \times 2 = 20$ for the OGB datasets).

4.5. Analyses on Layer-Wise Representations (RQ2)

We analyzed the layer-wise graph representations to investigate the effectiveness of the MLAP architecture. First, we computed the layer-wise graph representations and the final graph representation after MLAP aggregation for each graph in the datasets. We conducted two different analyses on these embedded representations.

4.5.1. t-SNE Visualization

We visualized the distribution of those representations in a two-dimensional space using t-SNE (van der Maaten & Hinton, 2008). The t-SNE hyperparameters were as follows: the learning rate was 50, the number of iterations was 3000, and the perplexity was 20.

4.5.2. Training Layer-Wise Classifiers

We trained layer-wise classifiers to evaluate the *goodness* of the layer-wise representations quantitatively. We followed the classifier implementations in Eqs. (12) and (13), but the graph representation terms \mathbf{h}_G in those equations were replaced by the layer-wise representations $\mathbf{h}_G^{(l)}$. These classifiers were trained on the representations of the training set. The classification performances were tested against the representations of the validation set. The classifiers were optimized by the Adam optimizer for 30 epochs with setting the learning rate to 10^{-3} .

5. Results

5.1. Model Performances

We summarize the performance of each architecture in Table 1.

5.1.1. Synthetic Dataset

Fig. 4 shows the performance of each architecture for each network depth evaluated on the validation set in the synthetic dataset².

Under the bare GIN configuration, our MLAP architecture using the sum aggregator achieved the best performance (Error = 0.1930 ± 0.0093 [mean \pm s.e.]) with

²For legibility, we only plotted the results of naive architecture, the best one among four JK architectures, and the best one between two MLAP architectures in Figs. 4–6. The full results are available in Appendix A.

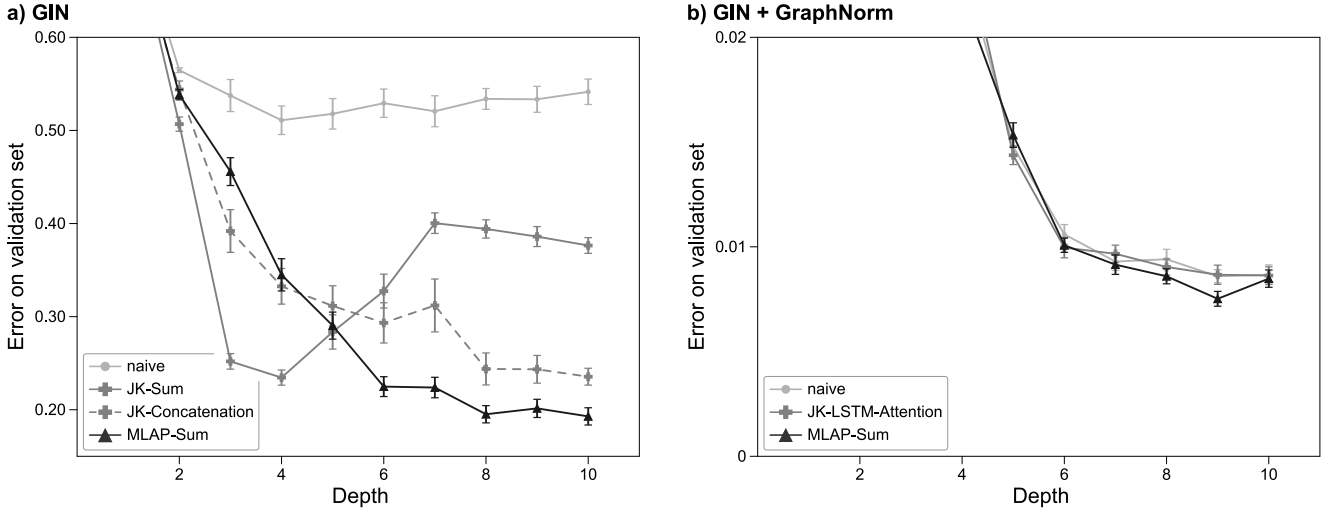


Figure 4: The performances for the synthetic dataset. a) GIN, b) GIN + GraphNorm. Full results are in Appendix Tables A.1 and A.2.

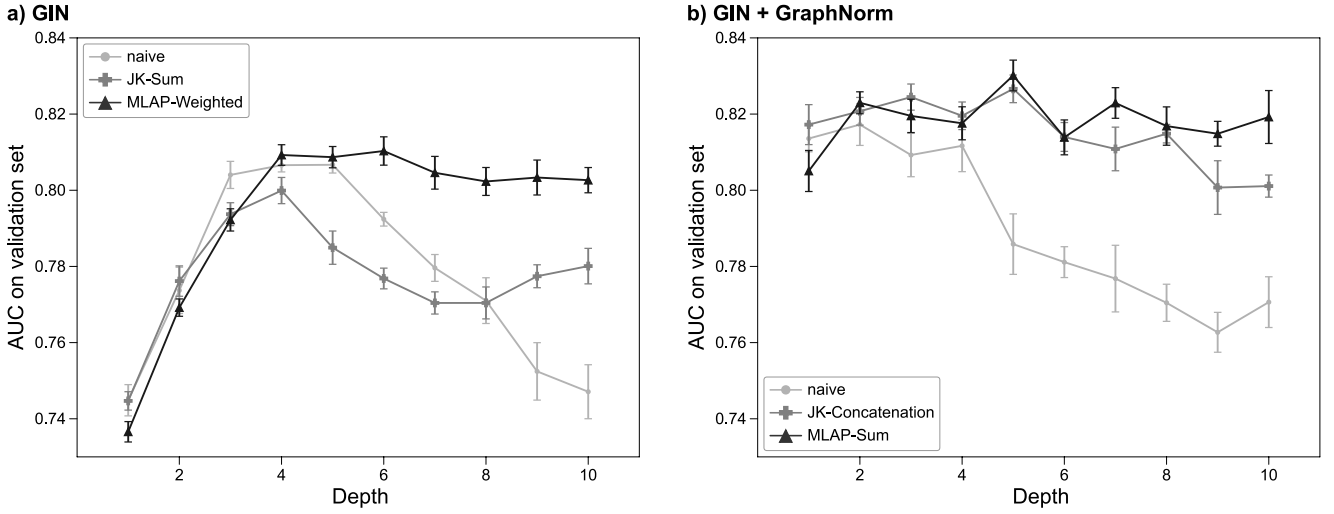


Figure 5: The performances for the ogbg-molhiv dataset. a) GIN, b) GIN + GraphNorm. Full results are in Appendix Tables A.3 and A.4.

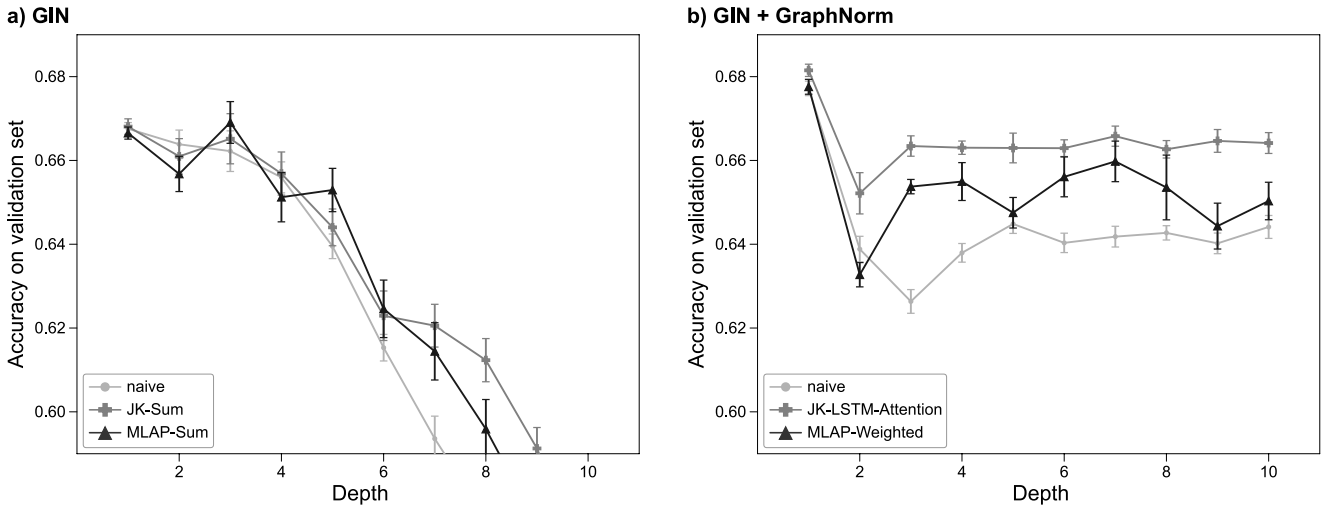


Figure 6: The performances for the ogbg-ppa dataset. a) GIN, b) GIN + GraphNorm. Full results are in Appendix Tables A.5 and A.6.

Configuration	Architecture	Synthetic	ogbg-molhiv	ogbg-ppa
GIN	naive	0.5116 ± 0.0154 (4)	0.8067 ± 0.0022 (5)	0.6676 ± 0.0015 (1)
	JK-Sum	0.2347 ± 0.0082 (4)	0.7999 ± 0.0034 (4)	0.6681 ± 0.0018 (1)
	JK-Concatenation	0.2357 ± 0.0091 (10)	0.7830 ± 0.0039 (3)	0.6666 ± 0.0024 (1)
	JK-MaxPool	0.2779 ± 0.0183 (4)	0.7763 ± 0.0026 (2)	0.6668 ± 0.0016 (1)
	JK-LSTM-Attention	0.4109 ± 0.0215 (7)	0.7849 ± 0.0029 (8)	0.6667 ± 0.0015 (1)
	MLAP-Sum	$^{*}0.1930 \pm 0.0093$ (10)	0.8066 ± 0.0040 (3)	$^{*}0.6691 \pm 0.0050$ (3)
	MLAP-Weighted	0.2836 ± 0.0174 (6)	$^{*}0.8103 \pm 0.0037$ (6)	0.6687 ± 0.0013 (1)
GIN + GraphNorm	naive	0.0086 ± 0.0003 (9)	0.8172 ± 0.0055 (2)	0.6772 ± 0.0017 (1)
	JK-Sum	0.0096 ± 0.0004 (9)	0.8176 ± 0.0047 (3)	0.6797 ± 0.0024 (1)
	JK-Concatenation	0.0094 ± 0.0005 (7)	0.8266 ± 0.0036 (5)	0.6700 ± 0.0026 (1)
	JK-MaxPool	0.0089 ± 0.0004 (9)	0.8191 ± 0.0047 (3)	0.6760 ± 0.0021 (1)
	JK-LSTM-Attention	0.0086 ± 0.0004 (10)	0.8172 ± 0.0044 (2)	$^{*}0.6815 \pm 0.0015$ (1)
	MLAP-Sum	$^{*}0.0075 \pm 0.0004$ (9)	$^{*}0.8301 \pm 0.0040$ (5)	0.6783 ± 0.0015 (1)
	MLAP-Weighted	0.0100 ± 0.0004 (9)	0.8129 ± 0.0043 (5)	0.6776 ± 0.0018 (1)

Table 1: The summary of model performances. Each cell shows the best performance of an architecture for a dataset in *mean \pm standard error*. The number in parenthesis is the depth of the best model.

Configuration	Comparison	Synthetic			ogbg-molhiv			ogbg-ppa		
		z	p	E.S.	z	p	E.S.	z	p	E.S.
GIN	MLAP vs. naive	6.65	$^{*} < 10^{-5}$	0.859	0.832	0.214	0.186	1.66	0.052	0.372
	MLAP vs. JK	3.14	$^{*} < 10^{-3}$	0.406	1.97	$^{*} 0.027$	0.439	1.36	0.093	0.304
GIN + GraphNorm	MLAP vs. naive	1.94	$^{*} 0.025$	0.250	1.74	$^{*} 0.044$	0.389	0.529	0.312	0.118
	MLAP vs. JK	2.17	$^{*} 0.014$	0.280	0.378	0.367	0.085	-1.32	0.099	-0.296

Table 2: The statistical analysis results. We compared the best performance among MLAP models to naive models and JK models. z : z value computed in Mann-Whitney U -test. p : p -value of the U -test. * : significant difference. E.S.: effect size r . Note that the negative values for the ogbg-ppa dataset in the GIN + GraphNorm configuration mean JK was better than MLAP. See the main text for the detail.

$L = 10$. It outperformed the JK models: 0.2347 ± 0.0082 for 4-layer JK-Sum or 0.2357 ± 0.0091 for 10-layer JK-Concatenation. In other words, the error rate was decreased by 17.8% by the proposed method.

Under the GIN + GraphNorm configuration, the 9-layer MLAP-Sum model performed the best (0.0075 ± 0.0004). It was better than the best performance of the baseline models: 0.0086 ± 0.0003 for 9-layer naive model. That is, the error rate was decreased by 12.5%.

Under both configurations, the statistical tests showed that MLAP performed significantly better than the naive and the JK architectures (Table 2). The effect sizes (0.25–0.86) are regarded as moderate to large, according to the classification given in Cohen (1988, Section 3.2).

5.1.2. ogbg-molhiv

Fig. 5 shows the performances of the models evaluated on the validation set in the ogbg-molhiv dataset.

Under the GIN configuration, the 6-layer MLAP-Weighted model performed the best ($AUC = 0.8103 \pm 0.0037$). It was better than the best performance of the baseline models: 0.8067 ± 0.0022 for 5-layer naive model. The statistical tests showed that MLAP performed significantly better than JK, and there was a moderate to large effect size (0.439). On the other hand, the difference between MLAP and naive models was not significant, whereas the effect size (0.186) was small to moderate.

Under the GIN + GraphNorm configuration, the best performance was achieved by the 5-layer MLAP-Sum model

(0.8301 ± 0.0040). Again, this was better than the best baseline model (5-layer JK-Concatenation, 0.8266 ± 0.0036). The statistical tests showed that MLAP performed significantly better than naive models with a moderate effect size (0.389). However, the difference between MLAP and JK was not significant, and the effect size was small (0.085).

5.1.3. ogbg-ppa

Fig. 6 shows the results of the ogbg-ppa experiments.

Under the GIN configuration, the 3-layer MLAP-Sum model performed the best (Accuracy = 0.6691 ± 0.0050). MLAP-Sum was the only architecture that the performance of a multi-layer model was better than the single-layer model. The best baseline performance was 0.6681 ± 0.0018 (1-layer JK-Sum). Although the differences between MLAP and the baseline models were not significant, there existed moderate effect sizes (0.372 and 0.304).

Under GIN + GraphNorm configuration, the single-layer model performed the best within each architecture. The best performance was 0.6815 ± 0.0015 (1-layer JK-LSTM-Attention).

5.2. Analyses on Layer-Wise Representations

5.2.1. Synthetic Dataset

We visualized the learned layer-wise and the aggregated graph representations with a 10-layer MLAP-Sum model, whose validation error rate was 0.9056 (Fig. 7). There are $3 \times 3 = 9$ classes of graphs in this dataset,

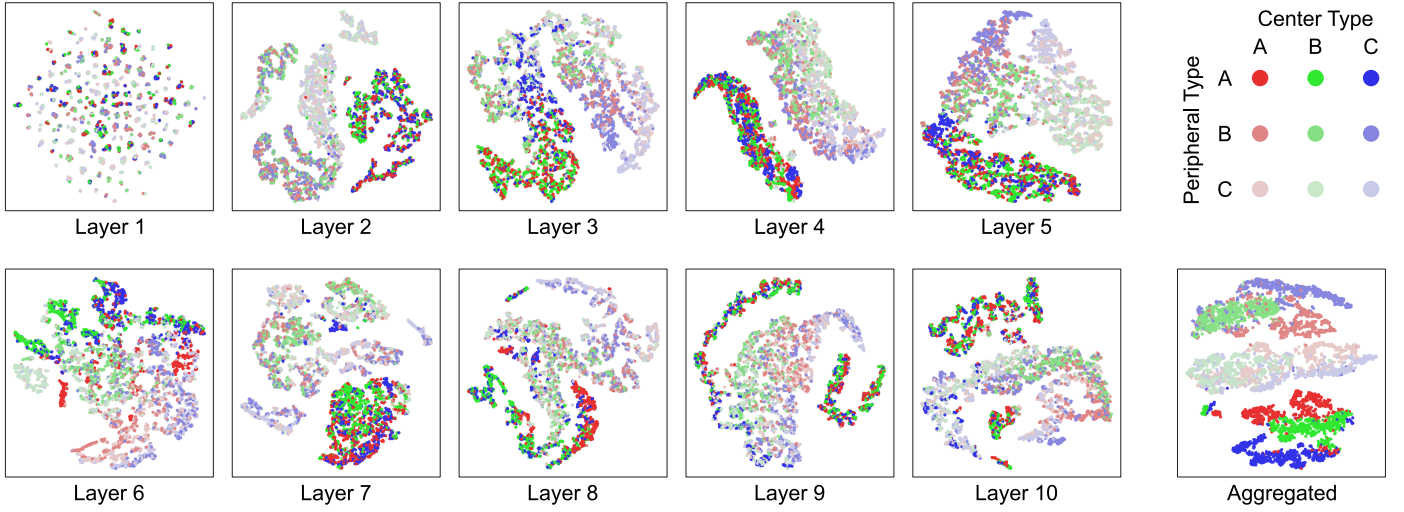


Figure 7: The layer-wise graph representations for the graphs in the synthetic dataset. They are visualized in two-dimensional spaces using t-SNE. Dots in each color represent samples in a class. (For interpretation of the reference to color in this figure legend, the reader is referred to the web version of this article.)

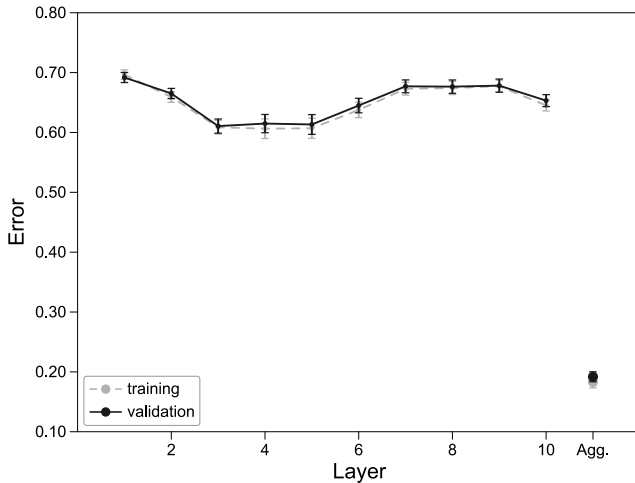


Figure 8: The classification performances of the layer-wise representations computed for the graphs in the synthetic dataset. The “Agg.” in the horizontal axis indicates the classifier’s performance trained with the graph representations after MLAP aggregation.

determined by the combination of the center component type and the peripheral component type (top-right panel in Fig. 7). The representations in the lower layers are highly discriminative for the *peripheral* types shown by the brightness of the dots. On the other hand, the representations in the higher layers, particularly Layer 6–8, are discriminative for the *center* types shown by the hue (*i.e.*, red, green, and blue). The aggregated representations are clearly discriminative for both the center and the peripheral types.

We quantitatively evaluated this observation using layer-wise classifiers for all trained 10-layer models with 30 different random seeds. Fig. 8 shows the layer-wise classification performance. Although the error rate for each

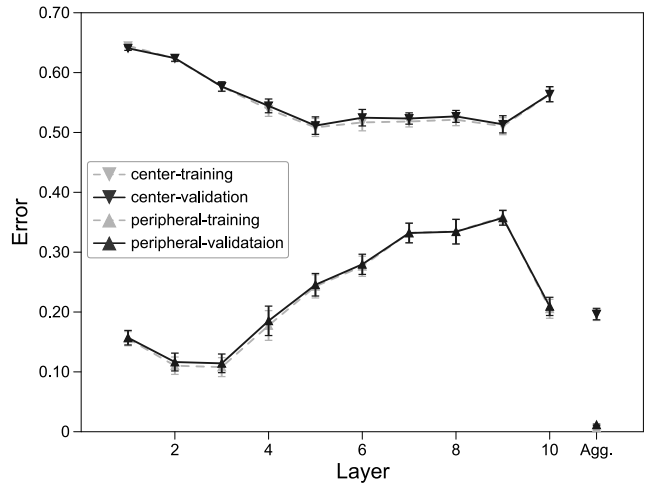


Figure 9: The classification performances of the layer-wise representations computed for the graphs in the synthetic dataset. Instead of the 9-class classification, they are trained independently for the center type (three classes) or the peripheral types (three classes). The “Agg.” in the horizontal axis indicates the classifier’s performance trained with the graph representations after MLAP aggregation.

layer-wise representation was not under 0.60, the aggregated representation by MLAP achieved the error rate of 0.1919 ± 0.0083 .

In addition to the 9-class classifiers, Fig. 9 shows the layer-wise classification performance under the *3-class* settings—each classifier was trained to predict either the center type or the peripheral type. The results in Fig. 9 show the discriminability among three *peripheral* types had the peak at Layer 2–3, whereas the discriminability among *center* types was better in higher layers (Layer 5–9). The 9-class classification performance (Fig. 8) has its peak in middle layers (Layer 3–5), which is right in between the two

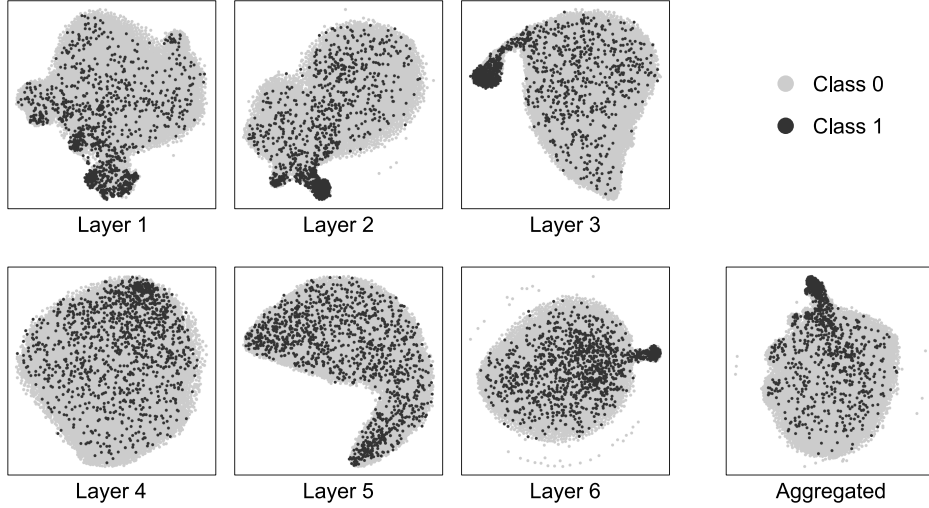


Figure 10: The layer-wise graph representations for ogbg-molhiv graphs. They are visualized in two-dimensional spaces using t-SNE. Each gray dot represents a *negative* sample, while each black dot represents a *positive* sample.

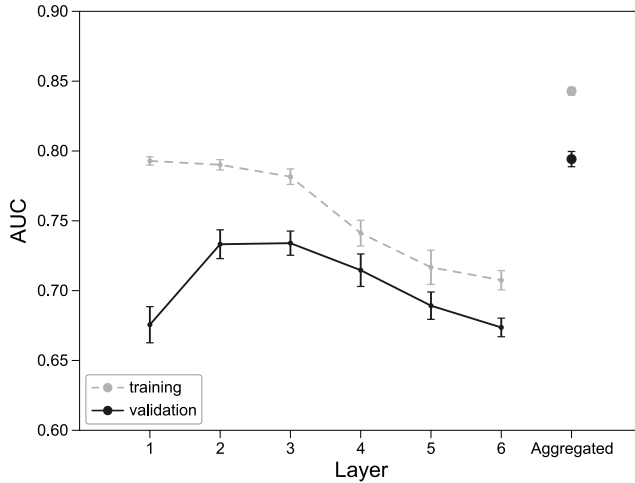


Figure 11: The classification performances of the layer-wise representations computed for ogbg-molhiv graphs. The “Aggregated” in the horizontal axis indicates the classifier’s performance trained with the graph representations after MLAP aggregation.

3-class classifiers. These results are consistent with the qualitative observation in Fig. 7.

5.2.2. *ogbg-molhiv*

In Fig. 10, We visualized the layer-wise representations by a 6-layer MLAP-Weighted model trained with the ogbg-molhiv dataset, whose validation AUC score was 0.8242. Each gray dot represents a *negative* sample, while each black dot represents a *positive* sample. The discriminability between the two classes was better in the lower layers, and it degrades toward the higher layers. However, aggregating those representations by taking weighted sum produces a more localized sample distribution than any representations in the intermediate layers.

The analysis using the layer-wise classifiers supports

the intuition obtained from the t-SNE visualization. Fig. 11 shows the training and validation AUC scores for each layer-wise classifier. The best validation score among the intermediate layers (0.7340 ± 0.0087) was marked at $l = 3$, but the score after MLAP aggregation is better than any intermediate layers (0.7942 ± 0.0055).

5.2.3. *ogbg-ppa*

Fig. 12 shows the t-SNE visualization results of the layer-wise representation by a 3-layer MLAP-Sum model (Accuracy = 0.6854). Layer 3 shows the best discriminative representation, while representations in Layer 1 and 2 do not seem clearly discriminative. Also, the discriminability in the MLAP-aggregated representation seems at a similar level to Layer 3.

The layer-wise classifier analysis also showed similar results (Fig. 13). The representations in $l = 3$ achieved the best validation score (0.6315 ± 0.0022). The score for the aggregated representations was slightly better (0.6497 ± 0.0031), but the effect of the MLAP architecture was not as big as seen in the other two datasets.

6. Discussion

In this study, we proposed the MLAP architecture for GNNs, which introduces layer-wise attentional graph pooling layers and computes the final graph representation by unifying the layer-wise graph representations. Experiments showed that our MLAP framework, which can utilize the structural information of graphs with multiple levels of localities, improved the classification performance in two out of three datasets. The performance of the *naive* architecture degraded as the number of layers increased. This is because the deep *naive* models lost the local structural information through many message passing steps due to oversmoothing. On the other hand, the

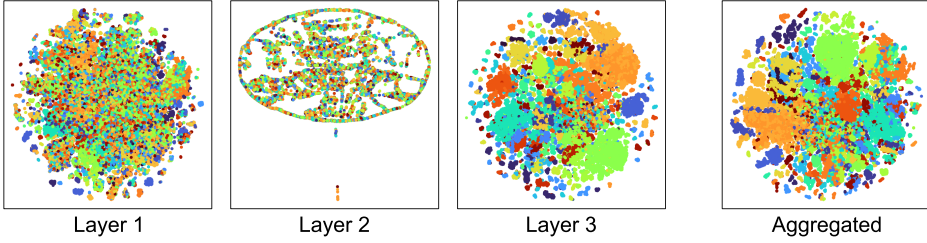


Figure 12: The layer-wise graph representations for ogbg-ppa graphs. They are visualized in two-dimensional spaces using t-SNE. Dots in each color represent samples in a class. (For interpretation of the reference to color in this figure legend, the reader is referred to the web version of this article.)

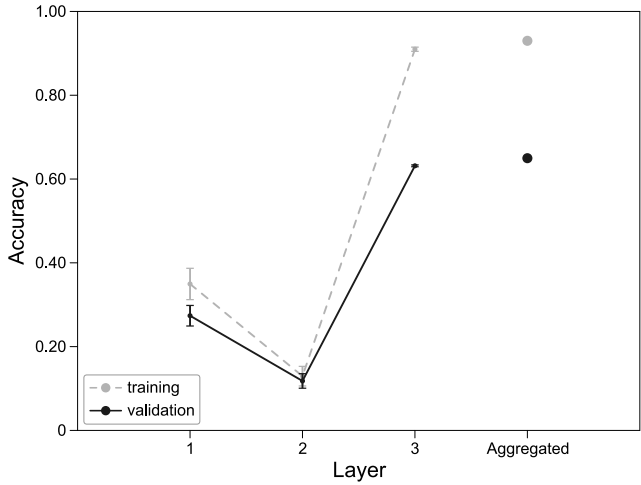


Figure 13: The classification performances of the layer-wise representations computed for ogbg-ppa graphs. The “Aggregated” in the horizontal axis indicates the classifier’s performance trained with the graph representations after MLAP aggregation.

difference in performance between *MLAP* and *JK* would be because of the operation order between the graph pooling and the information aggregation from multiple levels of localities. *MLAP* computes the graph representations by $f_{\text{agg}}\left(\text{Pool}^{(l)}(\mathbf{h}_n^{(l)})\right)$, whereas *JK* computes them by $\text{Pool}\left(f_{\text{JK}}(\mathbf{h}_n^{(l)})\right)$. Since *JK* aggregates the node representations in multiple levels of localities *before* the pooling, it might be difficult for the attention mechanism to learn which node to focus on. That is, structural information in a specific locality might be squashed before the pooling operation. In contrast, the *MLAP* architecture can tune the attention on nodes specifically in each information locality because it preserves the representations in each locality independently.

The analyses on the layer-wise graph representations supported our motivation behind *MLAP*—GNN performance can be improved by aggregating representations in different levels of localities. In the analyses using the synthetic dataset, the discriminability of the representations in the higher layers was worse than those in the lower layers (Fig. 8). However, using 3-class classifier analyses, we

showed that the learned representations have better discriminability of the *peripheral* types in the lower layers, whereas the discriminability of the *center* type is better in higher layers. These results indicate that, even though the apparent classification performance in higher layers is low, those layers do have essential information to classify the graphs in this dataset correctly. Aggregating layer-wise representations from multiple steps of message passing has the potential to reflect all the necessary information from various levels of localities in the final graph representation, leading to performance improvement. The results with the ogbg-molhiv dataset also showed that the *MLAP*-aggregated representation had better discriminability than any layer-wise representations. This would be because biochemical molecule graphs have commonly observed patterns—carbohydrate chains and amino groups, *etc.*—and the function of a molecule is determined by the combination of these substructures. The *MLAP* architecture would effectively capture such patterns in lower layers and their combinations in higher layers. On the other hand, the *MLAP* architecture did not work well for the ogbg-ppa dataset. This might be caused by how the dataset was generated: each graph in this dataset is a *subgraph* of a gigantic biochemical protein-protein association (PPA) graph. Although PPA graphs are known to have fractal characteristics (Kim et al., 2007), for which aggregating multi-locality features would be beneficial, subsampling from the original PPA graph can destroy such characteristics and impair the advantage of *MLAP*.

An advantage of the aggregation mechanism of the layer-wise representations (*i.e.*, both *JK* and *MLAP*) is that such a mechanism can coincide with almost any kind of other GNN techniques. For example, one can apply *JK* or *MLAP* for any backbone GNN architecture (GCN, GIN, GAT, *etc.*). Also, they can co-exist with the residual connection architectures or normalization techniques as well. The aggregation mechanism potentially improves the performance of GNN models coordinately with these techniques. Actually, multiple prior GRL studies have adopted *JK* architecture in their models and reported performance improvement. In this study, we follow the idea to aggregate layer-wise representations, and we showed that combining the aggregation mechanism with layer-wise attention pooling can further improve the learned graph rep-

resentation for graph-level classification tasks. Our experimental results validated that MLAP can be used with GraphNorm (Cai et al., 2020) and the learned representation became more discriminative.

Another interesting observation is that *MLAP-Weighted* performed worse than *MLAP-Sum* in some datasets. We speculate that having weight parameters for layers in the aggregation process might induce instability in the training phase. Appendix B provides preliminary results supporting this hypothesis. We will continue analyzing the cause of this phenomenon, and it might provide new insights toward further improvements in the MLAP architecture.

Designing neural network architectures by adopting knowledge in neuroscience is a popular research topic. The multi-level attention mechanism introduced in the MLAP architecture can also be seen as an analogy of the attention mechanism in the cognitive system of humans or other primates. Such cognitive systems, particularly the visual perception mechanism, is hierarchically organized and accompanied by hierarchical attention mechanisms. For example, the ventral visual pathway contributes to the hierarchical computation of object recognition mechanisms (Kravitz et al., 2013). In the ventral visual pathway, the neural information in the area V1 represents the raw visual inputs, and the representations are hierarchically abstracted towards the inferior temporal cortices as the receptive field—*i.e.*, locality—of the information is expanded. DeWeerd et al. (1999) found that lesions in the cortical areas V4 and TEO, both of which are components in the ventral pathway, contribute to the attentional processing in receptive fields with different sizes. As an example of artificial neural network studies inspired by these neuroscience studies, Taylor et al. (2009) proposed a method to autonomously control a robot using a neural network model with a hierarchical attention system, in which goal-oriented attention signals mediates the behavior of the network. Brain-inspired neural network architecture would improve the performance or the efficiency of the models, whereas the computational studies on neural networks might contribute back to neuroscience research. Hence, neuroscience and artificial neural network will keep on affecting mutually and developing along with each other.

There are several possible directions to further extend the proposed methods. First, exploring other aggregator functions than those proposed in this study, *i.e.*, *sum* and *weighted*, is needed. For example, it is possible to design an aggregator that models the relationships among layer-wise representations, whereas the proposed aggregators treated the layer-wise representations as independent of each other. Also, one can design an aggregator that only uses the representations in a subset of layers to reduce the computational cost, although the proposed aggregators required the layer-wise representations in all of the GNN layers. Second, multi-stage training of the models with MLAP architecture would be beneficial. Instead of training the entire GNN models with MLAP at once,

as we did in this study, one can train the GNN backbone without MLAP first and then fine-tune the model with the MLAP. This kind of multi-stage training would stabilize the learning process, particularly when using the MLAP with an aggregator that has additional trainable parameters, like the *MLAP-Weighted* architecture. Lastly, our MLAP architecture would be adopted to arbitrary deep learning models, even not limited to GNNs. For example, convolutional neural networks (CNNs) for computer vision would be good candidates. Some CNN studies, such as U-Net (Ronneberger et al., 2015), have already considered the hierarchy of the information processed in the neural networks. Adopting the hierarchical attention mechanism to such models might improve their performance.

7. Conclusion

In this study, we proposed the MLAP architecture for GNN models that aggregates graph representations in multiple levels of localities. The results suggest that the proposed architecture is effective to learn graph representations with high discriminability. There are many kinds of real-world networks whose properties are represented in the substructures with multiple levels of localities, and applying MLAP would improve the performances of GRL models for those graphs.

Conflict of Interest

The authors declare no competing financial interests.

Acknowledgements

We thank Y. Ikutani for his valuable comments. This work was supported by JSPS KAKENHI grant number 16H06569, 18K18108, 18K19821, and JP19J20669.

References

- Ahmed, A., Shervashidze, N., Narayananamurthy, S. M., Josifovski, V., & Smola, A. J. (2013). Distributed large-scale natural graph factorization. In *Proceedings of the 22nd International World Wide Web Conference* (pp. 37–48).
- Ba, L. J., Kiros, J. R., & Hinton, G. E. (2016). Layer normalization. *arXiv preprint, arXiv:1607.06450*.
- Bahdanau, D., Cho, K., & Bengio, Y. (2015). Neural machine translation by jointly learning to align and translate. In *Proceedings of the 3rd International Conference on Learning Representations*.
- Belkin, M., & Niyogi, P. (2001). Laplacian eigenmaps and spectral techniques for embedding and clustering. In *Advances in Neural Information Processing Systems 14* (pp. 585–591).
- Bruna, J., Zaremba, W., Szlam, A., & LeCun, Y. (2014). Spectral networks and locally connected networks on graphs. In *Proceedings of the 2nd International Conference on Learning Representations*.
- Cai, T., Luo, S., Xu, K., He, D., Liu, T., & Wang, L. (2020). Graph-Norm: A principled approach to accelerating graph neural network training. *arXiv preprint, arXiv:2009.03294*.
- Cangea, C., Velickovic, P., Jovanovic, N., Kipf, T., & Liò, P. (2018). Towards sparse hierarchical graph classifiers. *arXiv preprint, arXiv:1811.01287*.

Chen, M., Wei, Z., Huang, Z., Ding, B., & Li, Y. (2020). Simple and deep graph convolutional networks. In *Proceedings of the 37th International Conference on Machine Learning* (pp. 1725–1735).

Cohen, J. (1988). *Statistical power analysis for the behavioral sciences*. Academic press.

Defferrard, M., Bresson, X., & Vandergheynst, P. (2016). Convolutional neural networks on graphs with fast localized spectral filtering. In *Advances in Neural Information Processing Systems 29* (pp. 3837–3845).

Dehmmamy, N., Barabási, A., & Yu, R. (2019). Understanding the representation power of graph neural networks in learning graph topology. In *Advances in Neural Information Processing Systems 32* (pp. 15387–15397).

DeWeerd, P., Peralta, M. R., Desimone, R., & Ungerleider, L. G. (1999). Loss of attentional stimulus selection after extrastriate cortical lesions in macaques. *Nature Neuroscience*, 2, 753–758.

Duvenaud, D. K., Maclaurin, D., Iparragirre, J., Bombarell, R., Hirzel, T., Aspuru-Guzik, A., & Adams, R. P. (2015). Convolutional networks on graphs for learning molecular fingerprints. In *Advances in Neural Information Processing Systems 28* (pp. 2224–2232).

Gao, H., & Ji, S. (2019). Graph U-Nets. In *Proceedings of the 36th International Conference on Machine Learning* (pp. 2083–2092).

Gilmer, J., Schoenholz, S. S., Riley, P. F., Vinyals, O., & Dahl, G. E. (2017). Neural message passing for quantum chemistry. In *Proceedings of the 34th International Conference on Machine Learning* (pp. 1263–1272).

Gori, M., Monfardini, G., & Scarselli, F. (2005). A new model for learning in graph domains. In *Proceedings of the IEEE International Conference on Bioinformatics and Biomedicine*.

Hamilton, W. L. (2020). *Graph Representation Learning*. Morgan and Claypool.

Hamilton, W. L., Ying, R., & Leskovec, J. (2017a). Representation learning on graphs: Methods and applications. *IEEE Data Engineering Bulletin*, 40, 52–74.

Hamilton, W. L., Ying, Z., & Leskovec, J. (2017b). Inductive representation learning on large graphs. In *Advances in Neural Information Processing Systems 30* (pp. 1024–1034).

He, K., Zhang, X., Ren, S., & Sun, J. (2016). Deep residual learning for image recognition. In *Proceedings of the 2016 IEEE Conference on Computer Vision and Pattern Recognition* (pp. 770–778).

Hu, W., Fey, M., Zitnik, M., Dong, Y., Ren, H., Liu, B., Catasta, M., & Leskovec, J. (2020). Open graph benchmark: Datasets for machine learning on graphs. In *Advances in Neural Information Processing Systems 33* (pp. 22118–22133).

Ioffe, S., & Szegedy, C. (2015). Batch normalization: Accelerating deep network training by reducing internal covariate shift. In *Proceedings of the 32nd International Conference on Machine Learning* (pp. 448–456).

Kim, J., Goh, K.-I., Salvi, G., Oh, E., Kahng, B., & Kim, D. (2007). Fractality in complex networks: critical and supercritical skeletons. *Physical Review E*, 75, 016110.

Kingma, D. P., & Ba, J. (2015). Adam: A method for stochastic optimization. In *Proceedings of the 3rd International Conference on Learning Representations*.

Kipf, T. N., & Welling, M. (2017). Semi-supervised classification with graph convolutional networks. In *Proceedings of the 5th International Conference on Learning Representations*.

Kondor, R. I., & Lafferty, J. (2002). Diffusion kernels on graphs and other discrete structures. In *Proceedings of the 19th International Conference on Machine Learning* (pp. 315–322).

Kravitz, D. J., Saleem, K. S., Baker, C. I., Ungerleider, L. G., & Mishkin, M. (2013). The ventral visual pathway: an expanded neural framework for the processing of object quality. *Trends in Cognitive Sciences*, 17, 26–49.

Lee, J., Lee, I., & Kang, J. (2019). Self-attention graph pooling. In *Proceedings of the 36th International Conference on Machine Learning* (pp. 3734–3743).

Li, G., Müller, M., Thabet, A. K., & Ghanem, B. (2019). DeepGCNs: Can GCNs go as deep as CNNs? In *Proceedings of the 2019 IEEE/CVF International Conference on Computer Vision* (pp. 9266–9275).

Li, Q., Han, Z., & Wu, X. (2018). Deeper insights into graph convolutional networks for semi-supervised learning. In *Proceedings of the 32nd AAAI Conference on Artificial Intelligence* (pp. 3538–3545).

Li, Y., Tarlow, D., Brockschmidt, M., & Zemel, R. S. (2016). Gated graph sequence neural networks. In *Proceedings of the 4th International Conference on Learning Representations*.

van der Maaten, L., & Hinton, G. (2008). Visualizing data using t-SNE. *Journal of Machine Learning Research*, 9, 2579–2605.

Min, Y., Wenkel, F., & Wolf, G. (2020). Scattering GCN: overcoming oversmoothness in graph convolutional networks. In *Advances in Neural Information Processing Systems 33*.

Niepert, M., Ahmed, M., & Kutzkov, K. (2016). Learning convolutional neural networks for graphs. In *Proceedings of the 33rd International Conference on Machine Learning* (pp. 2014–2023).

Oono, K., & Suzuki, T. (2020). Graph neural networks exponentially lose expressive power for node classification. In *Proceedings of the 8th International Conference on Learning Representations*.

Page, L., Brin, S., Motwani, R., & Winograd, T. (1999). *The PageRank Citation Ranking: Bringing Order to the Web*. Technical Report 1999-66 Stanford InfoLab.

Ranjan, E., Sanyal, S., & Talukdar, P. P. (2020). ASAP: adaptive structure aware pooling for learning hierarchical graph representations. In *Proceedings of the 34th AAAI Conference on Artificial Intelligence* (pp. 5470–5477).

Rong, Y., Huang, W., Xu, T., & Huang, J. (2020). Dropedge: Towards deep graph convolutional networks on node classification. In *Proceedings of the 8th International Conference on Learning Representations*.

Ronneberger, O., Fischer, P., & Brox, T. (2015). U-Net: Convolutional networks for biomedical image segmentation. In *Proceedings of the International Conference on Medical Image Computing and Computer-Assisted Intervention* (pp. 234–241).

Scarselli, F., Gori, M., Tsoi, A. C., Hagenbuchner, M., & Monfardini, G. (2009). The graph neural network model. *IEEE Transactions on Neural Networks*, 20, 61–80.

Shervashidze, N., Schweitzer, P., van Leeuwen, E. J., Mehlhorn, K., & Borgwardt, K. M. (2011). Weisfeiler-Lehman graph kernels. *Journal of Machine Learning Research*, 12, 2539–2561.

Szklarczyk, D., Gable, A. L., Lyon, D., Junge, A., Wyder, S., Huerta-Cepas, J., Simonovic, M., Doncheva, N. T., Morris, J. H., Bork, P., Jensen, L. J., & Mering, C. (2018). STRING v11: protein–protein association networks with increased coverage, supporting functional discovery in genome-wide experimental datasets. *Nucleic Acids Research*, 47, D607–D613.

Taylor, J. G., Hartley, M., Taylor, N., Panchev, C., & Kasderidis, S. (2009). A hierarchical attention-based neural network architecture, based on human brain guidance, for perception, conceptualisation, action and reasoning. *Image and Vision Computing*, 27, 1641–1657.

Veličković, P., Cucurull, G., Casanova, A., Romero, A., Liò, P., & Bengio, Y. (2018). Graph attention networks. In *Proceedings of the 6th International Conference on Learning Representations*.

Vinyals, O., Bengio, S., & Kudlur, M. (2016). Order matters: Sequence to sequence for sets. In *Proceedings of the 4th International Conference on Learning Representations*.

Wang, X., He, X., Cao, Y., Liu, M., & Chua, T. (2019). KGAT: knowledge graph attention network for recommendation. In *Proceedings of the 25th ACM SIGKDD International Conference on Knowledge Discovery & Data Mining* (pp. 950–958).

Wu, Z., Pan, S., Chen, F., Long, G., Zhang, C., & Yu, P. S. (2021). A comprehensive survey on graph neural networks. *IEEE Transactions on Neural Networks and Learning Systems*, 32, 4–24.

Wu, Z., Ramsundar, B., Feinberg, E. N., Gomes, J., Geniesse, C., Pappu, A. S., Leswing, K., & Pande, V. (2018). MoleculeNet: a benchmark for molecular machine learning. *Chemical Science*, 9, 513–530.

Xu, K., Hu, W., Leskovec, J., & Jegelka, S. (2019). How powerful are graph neural networks? In *Proceedings of the 7th International Conference on Learning Representations*.

Xu, K., Li, C., Tian, Y., Sonobe, T., Kawarabayashi, K., & Jegelka, S. (2018). Representation learning on graphs with jumping knowledge networks. In *Proceedings of the 35th International Conference on Machine Learning* (pp. 5453–5462). volume 80.

Ying, Z., You, J., Morris, C., Xiang, R., , Hamilton, W. L., & Leskovec, J. (2018). Hierarchical graph representation learning with differentiable pooling. In *Advances in Neural Information Processing Systems 31* (pp. 4805–4815).

Zhang, J., & Meng, L. (2019). GResNet: Graph residual network for reviving deep gnns from suspended animation. *arXiv preprint, arXiv:1909.05729*.

Zhang, M., Cui, Z., Neumann, M., & Chen, Y. (2018a). An end-to-end deep learning architecture for graph classification. In *Proceedings of the 32nd AAAI Conference on Artificial Intelligence* (pp. 4438–4445).

Zhang, Z., Cui, P., & Zhu, W. (2018b). Deep learning on graphs: A survey. *arXiv preprint, arXiv:1812.04202*.

Zhao, L., & Akoglu, L. (2020). PairNorm: Tackling oversmoothing in gnns. In *Proceedings of the 8th International Conference on Learning Representations*.

Zhou, K., Dong, Y., Wang, K., Lee, W. S., Hooi, B., Xu, H., & Feng, J. (2020a). Understanding and resolving performance degradation in graph convolutional networks. *arXiv preprint, arXiv:2006.07107*.

Zhou, K., Huang, X., Li, Y., Zha, D., Chen, R., & Hu, X. (2020b). Towards deeper graph neural networks with differentiable group normalization. In *Advances in Neural Information Processing Systems 33*.

Appendix A. Full Results of Model Performance Evaluation

In Figs. 4–6, we only plotted the results of naive architecture, the best one among four JK architectures, and the best one between two MLAP architectures, for legibility. Here, we provide the full results in Tables A.1–A.6 (next page).

Appendix B. Why MLAP-Weighted perform worse than MLAP-Sum in some datasets?

In the synthetic dataset and ogbg-ppa, the *MLAP-Weighted* architecture performed worse than *MLAP-Sum*. However, intuitively, taking balance across layers using the weight parameters sounds reasonable and effective. In this appendix section, we show the results of preliminary analyses on the cause of this phenomenon.

Fig. B.1 shows the weight values in the trained models with 30 different random seeds for the synthetic dataset, and Fig. B.2 shows the weights in ogbg-molhiv models 10 seeds. The weight values for the synthetic dataset, where MLAP-Weighted was inferior to MLAP-Sum, have big variances, and the weight distribution covers the “constant weight” line (dashed horizontal line; an MLAP-Weighted model is virtually equivalent to an MLAP-Sum model if the weight parameters are equal to this value). It is expected that the desirable weight for each layer is not largely different from the constant weight. On the other hand, having such weight parameters with big variance indicates instability during the model training.

In contrast, the weight values for ogbg-molhiv, where MLAP-Weighted performed better than MLAP-Sum, have smaller variances, and the distribution deviates from the constant weight line, particularly in Layers 1 and 6. It is expected that the desirable weight for those layers is indeed different from the constant weight, and the model might adapt to the balance across layers.

This preliminary analysis suggests that, depending on some properties of datasets, the *MLAP-Weighted* architecture can excel *MLAP-Sum*. We will continue working on the analyses to identify the suitability of each MLAP aggregator to a certain dataset.

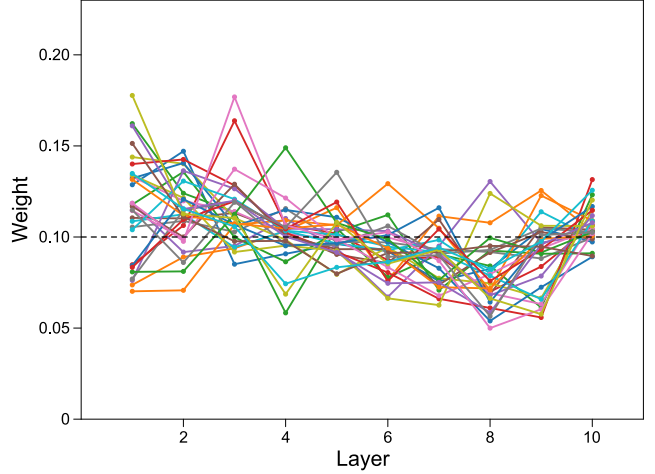


Figure B.1: Weight parameters of 10-layer MLAP-Weighted models trained for the synthetic dataset. A line shows the weight vector in a model (30 lines in total). The dashed horizontal line shows the weight if all layers contribute to the final graph representation equally.

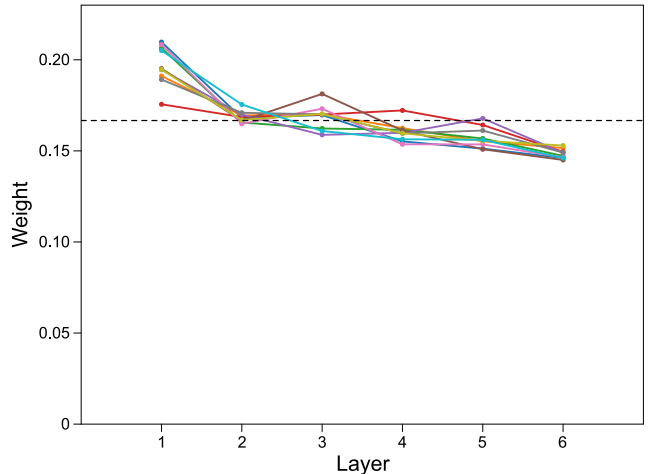


Figure B.2: Weight parameters of 6-layer MLAP-Weighted models trained for the ogbg-molhiv dataset. A line shows the weight vector in a model (10 lines in total). The dashed horizontal line shows the weight if all layers contribute to the final graph representation equally.

Configuration	Architecture	Number of Layers				
		1 6	2 7	3 8	4 9	5 10
GIN	naive	0.7426 \pm 0.0008	0.5654 \pm 0.0026	0.5382 \pm 0.0173	0.5116 \pm 0.0154	0.5186 \pm 0.0164
		0.5300 \pm 0.015	0.5213 \pm 0.0167	0.5346 \pm 0.0112	0.5342 \pm 0.0140	0.5423 \pm 0.0137
	JK-Sum	0.7418 \pm 0.0007	0.5074 \pm 0.0077	0.2521 \pm 0.0083	0.2347 \pm 0.0082	0.2838 \pm 0.0184
		0.3278 \pm 0.0183	0.4009 \pm 0.0111	0.3947 \pm 0.0098	0.3864 \pm 0.0107	0.3769 \pm 0.0084
	JK-Concatenation	0.7233 \pm 0.0081	0.5447 \pm 0.0092	0.3924 \pm 0.0230	0.3329 \pm 0.0192	0.3119 \pm 0.0216
		0.2936 \pm 0.0217	0.3123 \pm 0.0285	0.2440 \pm 0.0172	0.2436 \pm 0.0149	0.2357 \pm 0.0091
	JK-MaxPool	0.7384 \pm 0.0042	0.5314 \pm 0.0025	0.3304 \pm 0.0074	0.2779 \pm 0.0183	0.3240 \pm 0.0177
	JK-LSTM-Attention	0.3441 \pm 0.0175	0.3678 \pm 0.0172	0.3969 \pm 0.0132	0.4163 \pm 0.0112	0.4229 \pm 0.0116
MLAP	MLAP-Sum	0.7418 \pm 0.0008	0.5869 \pm 0.0119	0.4654 \pm 0.0202	0.4601 \pm 0.0198	0.4418 \pm 0.0169
		0.4199 \pm 0.0236	0.4109 \pm 0.0215	0.4204 \pm 0.0190	0.4126 \pm 0.0185	0.4530 \pm 0.0148
	MLAP-Weighted	0.7423 \pm 0.0009	0.5391 \pm 0.0055	0.4564 \pm 0.0150	0.3453 \pm 0.0173	0.2906 \pm 0.0145
	0.2250 \pm 0.0107	0.2240 \pm 0.0110	0.1953 \pm 0.0093	0.2016 \pm 0.0098	*0.1930 \pm 0.0093	
	MLAP-Weighted	0.7431 \pm 0.0007	0.5539 \pm 0.0088	0.4821 \pm 0.0181	0.4112 \pm 0.0198	0.3536 \pm 0.0197
	0.2836 \pm 0.0174	0.3029 \pm 0.0189	0.2896 \pm 0.0143	0.2908 \pm 0.0142	0.2861 \pm 0.0170	

Table A.1: Full results in the synthetic dataset experiments under GIN configuration. **bold**: best performance in an architecture, *****: the overall best performance.

Configuration	Architecture	Number of Layers				
		1 6	2 7	3 8	4 9	5 10
GIN + GraphNorm	naive	0.5846 \pm 0.0017	0.2763 \pm 0.0092	0.0597 \pm 0.0023	0.0237 \pm 0.0008	0.0148 \pm 0.0004
		0.0106 \pm 0.0005	0.0093 \pm 0.0004	0.0094 \pm 0.0005	0.0086 \pm 0.0003	0.0087 \pm 0.0005
	JK-Sum	0.5886 \pm 0.0019	0.2549 \pm 0.0054	0.0576 \pm 0.0014	0.0236 \pm 0.0007	0.0141 \pm 0.0004
		0.0106 \pm 0.0004	0.0109 \pm 0.0004	0.0099 \pm 0.0004	0.0096 \pm 0.0004	0.0097 \pm 0.0004
	JK-Concatenation	0.5880 \pm 0.0032	0.2634 \pm 0.0068	0.0554 \pm 0.0011	0.0225 \pm 0.0006	0.0172 \pm 0.0005
		0.0114 \pm 0.0004	0.0094 \pm 0.0005	0.0097 \pm 0.0004	0.0100 \pm 0.0005	0.0106 \pm 0.0004
	JK-MaxPool	0.5880 \pm 0.0020	0.3203 \pm 0.0025	0.0760 \pm 0.0011	0.0250 \pm 0.0007	0.0146 \pm 0.0005
	JK-LSTM-Attention	0.0110 \pm 0.0005	0.0090 \pm 0.0004	0.0091 \pm 0.0004	0.0089 \pm 0.0004	0.0090 \pm 0.0004
MLAP	MLAP-Sum	0.5874 \pm 0.0019	0.2693 \pm 0.0064	0.0615 \pm 0.0021	0.0251 \pm 0.0010	0.0144 \pm 0.0004
		0.0100 \pm 0.0005	0.0097 \pm 0.0004	0.0090 \pm 0.0004	0.0087 \pm 0.0005	0.0086 \pm 0.0004
	MLAP-Weighted	0.5878 \pm 0.0019	0.2669 \pm 0.0075	0.0574 \pm 0.0018	0.0220 \pm 0.0011	0.0153 \pm 0.0006
	0.0101 \pm 0.0003	0.0091 \pm 0.0005	0.0086 \pm 0.0004	*0.0075 \pm 0.0004	0.0085 \pm 0.0004	
	0.5868 \pm 0.0018	0.2840 \pm 0.0090	0.0696 \pm 0.0021	0.0284 \pm 0.0006	0.0161 \pm 0.0006	
	0.0126 \pm 0.0005	0.0103 \pm 0.0004	0.0104 \pm 0.0004	0.0100 \pm 0.0004	0.0100 \pm 0.0005	

Table A.2: Full results in the synthetic dataset experiments under GIN + GraphNorm configuration. **bold**: best performance in an architecture, *****: the overall best performance.

Configuration	Architecture	Number of Layers				
		1 6	2 7	3 8	4 9	5 10
GIN	naive	0.7449 \pm 0.0041	0.7737 \pm 0.0061	0.8040 \pm 0.0036	0.8066 \pm 0.0018	0.8067 \pm 0.0022
		0.7924 \pm 0.0018	0.7796 \pm 0.0035	0.7710 \pm 0.0060	0.7524 \pm 0.0075	0.7471 \pm 0.0071
	JK-Sum	0.7447 \pm 0.0024	0.7761 \pm 0.0040	0.7937 \pm 0.0030	0.7999 \pm 0.0034	0.7849 \pm 0.0044
		0.7768 \pm 0.0027	0.7704 \pm 0.0029	0.7704 \pm 0.0042	0.7774 \pm 0.0030	0.7801 \pm 0.0047
	JK-Concatenation	0.7554 \pm 0.0036	0.7705 \pm 0.0021	0.7830 \pm 0.0039	0.7738 \pm 0.0028	0.7820 \pm 0.0034
		0.7730 \pm 0.0016	0.7739 \pm 0.0026	0.7725 \pm 0.0042	0.7711 \pm 0.0030	0.7686 \pm 0.0034
	JK-MaxPool	0.7447 \pm 0.0030	0.7763 \pm 0.0026	0.7675 \pm 0.0035	0.7715 \pm 0.0038	0.7759 \pm 0.0044
	JK-LSTM-Attention	0.7660 \pm 0.0040	0.7595 \pm 0.0029	0.7639 \pm 0.0025	0.7673 \pm 0.0026	0.7647 \pm 0.0028
MLAP	MLAP-Sum	0.7446 \pm 0.0041	0.7617 \pm 0.0033	0.7673 \pm 0.0019	0.7756 \pm 0.0027	0.7714 \pm 0.0032
		0.7735 \pm 0.0022	0.7775 \pm 0.0030	0.7849 \pm 0.0029	0.7829 \pm 0.0020	0.7745 \pm 0.0041
	MLAP-Weighted	0.7462 \pm 0.0025	0.7753 \pm 0.0047	0.8066 \pm 0.0040	0.8043 \pm 0.0037	0.8003 \pm 0.0044
	0.8004 \pm 0.0046	0.8046 \pm 0.0033	0.7991 \pm 0.0039	0.8019 \pm 0.0045	0.8006 \pm 0.0036	
	0.7366 \pm 0.0027	0.7692 \pm 0.0023	0.7922 \pm 0.0029	0.8092 \pm 0.0027	0.8087 \pm 0.0028	
	*0.8103 \pm 0.0037	0.8046 \pm 0.0043	0.8023 \pm 0.0037	0.8033 \pm 0.0046	0.8026 \pm 0.003	

Table A.3: Full results in the ogbg-molhiv experiments under GIN configuration. **bold**: best performance in an architecture, *****: the overall best performance.

Configuration	Architecture	Number of Layers				
		1 6	2 7	3 8	4 9	5 10
GIN + GraphNorm	naive	0.8136 \pm 0.0035	0.8172 \pm 0.0055	0.8093 \pm 0.0057	0.8117 \pm 0.0068	0.7859 \pm 0.0079
		0.7811 \pm 0.0041	0.7768 \pm 0.0087	0.7705 \pm 0.0049	0.7627 \pm 0.0052	0.7706 \pm 0.0067
	JK-Sum	0.8053 \pm 0.0048	0.8156 \pm 0.0021	0.8176 \pm 0.0047	0.8047 \pm 0.0053	0.8165 \pm 0.0026
		0.8056 \pm 0.0032	0.8072 \pm 0.0031	0.8109 \pm 0.0045	0.8126 \pm 0.0048	0.8065 \pm 0.0037
	JK-Concatenation	0.8172 \pm 0.0052	0.8207 \pm 0.0036	0.8245 \pm 0.0034	0.8195 \pm 0.0036	0.8266 \pm 0.0036
		0.8140 \pm 0.0038	0.8108 \pm 0.0057	0.8149 \pm 0.0024	0.8007 \pm 0.0070	0.8011 \pm 0.0029
	JK-MaxPool	0.8042 \pm 0.0051	0.8109 \pm 0.0039	0.8191 \pm 0.0047	0.8147 \pm 0.0073	0.8062 \pm 0.0041
		0.8071 \pm 0.0049	0.8062 \pm 0.0039	0.7932 \pm 0.0035	0.7960 \pm 0.0028	0.7891 \pm 0.0045
	JK-LSTM-Attention	0.7998 \pm 0.0033	0.8172 \pm 0.0044	0.8118 \pm 0.0044	0.8131 \pm 0.0068	0.8033 \pm 0.0057
		0.8088 \pm 0.0075	0.7997 \pm 0.0078	0.8102 \pm 0.0036	0.8023 \pm 0.0026	0.7915 \pm 0.0061
	MLAP-Sum	0.8051 \pm 0.0054	0.8230 \pm 0.0029	0.8195 \pm 0.0044	0.8176 \pm 0.0043	*0.8301 \pm 0.0040
		0.8139 \pm 0.0046	0.8229 \pm 0.0040	0.8169 \pm 0.0050	0.8148 \pm 0.0033	0.8192 \pm 0.0070
	MLAP-Weighted	0.8054 \pm 0.0043	0.8096 \pm 0.0050	0.8079 \pm 0.0049	0.8065 \pm 0.0036	0.8129 \pm 0.0043
		0.8071 \pm 0.0053	0.8014 \pm 0.0069	0.8054 \pm 0.0061	0.8029 \pm 0.0033	0.7987 \pm 0.0065

Table A.4: Full results in the ogbg-molhiv experiments under GIN + GraphNorm configuration. **bold**: best performance in an architecture, *****: the overall best performance.

Configuration	Architecture	Number of Layers				
		1 6	2 7	3 8	4 9	5 10
GIN	naive	0.6676 \pm 0.0015	0.6639 \pm 0.0034	0.6622 \pm 0.0048	0.6560 \pm 0.0037	0.6395 \pm 0.0029
		0.6153 \pm 0.0032	0.5936 \pm 0.0054	0.5746 \pm 0.0060	0.5442 \pm 0.0099	0.4973 \pm 0.0080
	JK-Sum	0.6681 \pm 0.0018	0.6610 \pm 0.0042	0.6652 \pm 0.0060	0.6569 \pm 0.0052	0.6440 \pm 0.0044
		0.6229 \pm 0.0059	0.6206 \pm 0.0051	0.6123 \pm 0.0052	0.5913 \pm 0.0050	0.5622 \pm 0.0090
	JK-Concatenation	0.6666 \pm 0.0024	0.6352 \pm 0.0041	0.6636 \pm 0.0100	0.6420 \pm 0.0057	0.6467 \pm 0.0066
		0.6257 \pm 0.0053	0.6219 \pm 0.0096	0.6152 \pm 0.0074	0.6011 \pm 0.0064	0.5876 \pm 0.0070
	JK-MaxPool	0.6668 \pm 0.0016	0.6076 \pm 0.0031	0.6049 \pm 0.0076	0.6070 \pm 0.0088	0.5962 \pm 0.0072
		0.6041 \pm 0.0057	0.6023 \pm 0.0061	0.5838 \pm 0.0055	0.5837 \pm 0.0075	0.5292 \pm 0.0104
	JK-LSTM-Attention	0.6667 \pm 0.0015	0.6127 \pm 0.0019	0.5910 \pm 0.0069	0.5888 \pm 0.0048	0.5542 \pm 0.0116
		0.5020 \pm 0.0333	0.4251 \pm 0.0452	0.4237 \pm 0.0479	0.4499 \pm 0.0265	0.3046 \pm 0.0305
	MLAP-Sum	0.6665 \pm 0.0014	0.6568 \pm 0.0042	*0.6691 \pm 0.0050	0.6512 \pm 0.0059	0.6529 \pm 0.0052
		0.6246 \pm 0.0069	0.6144 \pm 0.0068	0.5959 \pm 0.0071	0.5732 \pm 0.0106	0.5721 \pm 0.0074
	MLAP-Weighted	0.6687 \pm 0.0013	0.6463 \pm 0.0034	0.6542 \pm 0.0078	0.6358 \pm 0.0038	0.6305 \pm 0.0047
		0.6192 \pm 0.0046	0.6023 \pm 0.0079	0.5642 \pm 0.0065	0.5583 \pm 0.0096	0.5053 \pm 0.0155

Table A.5: Full results in the ogbg-ppa experiments under GIN configuration. **bold**: best performance in an architecture, *****: the overall best performance.

Configuration	Architecture	Number of Layers				
		1 6	2 7	3 8	4 9	5 10
GIN + GraphNorm	naive	0.6772 \pm 0.0017	0.6388 \pm 0.0031	0.6263 \pm 0.0028	0.6379 \pm 0.0022	0.6448 \pm 0.0023
		0.6403 \pm 0.0023	0.6418 \pm 0.0025	0.6427 \pm 0.0017	0.6402 \pm 0.0025	0.6441 \pm 0.0027
	JK-Sum	0.6797 \pm 0.0024	0.6408 \pm 0.0025	0.6370 \pm 0.0034	0.6414 \pm 0.0046	0.6415 \pm 0.0045
		0.6291 \pm 0.0020	0.6315 \pm 0.0039	0.6254 \pm 0.0027	0.6295 \pm 0.0026	0.6274 \pm 0.0032
	JK-Concatenation	0.6700 \pm 0.0026	0.6496 \pm 0.0039	0.6537 \pm 0.0032	0.6517 \pm 0.0040	0.6491 \pm 0.0025
		0.6516 \pm 0.0036	0.6466 \pm 0.0035	0.6465 \pm 0.0034	0.6479 \pm 0.0032	0.6429 \pm 0.0030
	JK-MaxPool	0.6760 \pm 0.0021	0.6475 \pm 0.0021	0.6415 \pm 0.0029	0.6446 \pm 0.0034	0.6349 \pm 0.0015
		0.6362 \pm 0.0040	0.6313 \pm 0.0030	0.6316 \pm 0.0039	0.6382 \pm 0.0055	0.6353 \pm 0.0037
	JK-LSTM-Attention	*0.6815 \pm 0.0015	0.6522 \pm 0.0049	0.6634 \pm 0.0024	0.6630 \pm 0.0016	0.6630 \pm 0.0035
		0.6629 \pm 0.0020	0.6658 \pm 0.0024	0.6627 \pm 0.0021	0.6647 \pm 0.0027	0.6642 \pm 0.0025
	MLAP-Sum	0.6783 \pm 0.0015	0.6373 \pm 0.0031	0.6362 \pm 0.0030	0.6370 \pm 0.0022	0.6353 \pm 0.0030
		0.6377 \pm 0.0042	0.6326 \pm 0.0026	0.6336 \pm 0.0026	0.6359 \pm 0.0025	0.6377 \pm 0.0036
	MLAP-Weighted	0.6776 \pm 0.0018	0.6327 \pm 0.0029	0.6538 \pm 0.0017	0.6550 \pm 0.0045	0.6475 \pm 0.0036
		0.6561 \pm 0.0048	0.6598 \pm 0.0048	0.6535 \pm 0.0077	0.6443 \pm 0.0055	0.6503 \pm 0.0045

Table A.6: Full results in the ogbg-ppa experiments under GIN + GraphNorm configuration. **bold**: best performance in an architecture, *****: the overall best performance.